Received: 14 April 2021 | Revised: 7 May 2021 | Accepted: 9 May 2021

DOI: 10.1111/jch.14298

ORIGINAL PAPER

WILEY

Cigarette smoking status alters dysbiotic gut microbes in hypertensive patients

Pan Wang MD | Ying Dong PhD | Jie Jiao MD | Kun Zuo MD | Chunming Han MD | Lei Zhao MD | Shu Ding MD | Xinchun Yang MD | Mulei Chen MD | Jing Li PhD

Heart Center & Beijing Key Laboratory of Hypertension, Beijing Chaoyang Hospital, Capital Medical University, Beijing, China

Correspondence
Jing Li and Mulei Chen, Heart Center, Beijing Key Laboratory of Hypertension, Beijing Chaoyang Hospital, Capital Medical University, 8th Gongtinanlu Rd, Chaoyang District, Beijing, China 100020.
Emails: lijing11999@163.com (J.L.); cml68@sina.cn (M.C.)

Funding information
This work was supported by the National Natural Science Foundation of China [grant numbers 81670214, 81870308, and 81970271]; the Beijing Natural Science Foundation [grant numbers 7172080]; and the National Nature Cultivation Fund of Beijing Chaoyang Hospital [grant numbers CHPY202050].

Abstract

Smoking not only is one of the most important risk factors of hypertension (HTN), but also alters the composition of gut microbiota (GM) in previous studies. Although dysbiosis of GM has been implicated in HTN, how GM alters in patients with HTN under smoking status is still not clear. This study aimed to explore the difference in intestinal microflora among smokers with HTN (S-HTN), nonsmokers with HTN (NS-HTN), and smokers without HTN (S-CTR) and identify whether cigarette smoking led to disordered intestinal microbiota in patients with HTN. Metagenomic sequencing analysis of fecal specimens was conducted in nonsmokers without HTN (NS-CTR, n = 9), S-CTR (n = 9), NS-HTN (n = 18), and S-HTN (n = 23). Compared with S-CTR or NS-HTN, the GM in S-HTN was disordered, with lower microbial α-diversity and significant difference of β-diversity on axes as compared to S-CTR at genus and species level. The microbial enterotype in S-HTN was inclined to *Prevotella*-dominant type. Dramatic changes in the intestinal genera and species composition were observed in S-HTN, including reduced enrichment of *Phycisphaera* and *Clostridium asparagiforme*. Moreover, the intestinal function altered in S-HTN. Therefore, the findings of the present study revealed GM disorders in S-HTN and clarified the role of smoking in impairing the intestinal microbiome in HTN. Tobacco control is particularly important for improving GM in patients with HTN, and might be beneficial in preventing future cardiovascular events.

1 | INTRODUCTION

Hypertension (HTN), the leading risk factor for cardiovascular disease (CVD), is responsible for nearly 9.4 million deaths annually worldwide.[1] An elevation in the blood pressure (BP) is clinically significantly associated with an increased risk of CVDs and other diseases, such as end-stage renal disease.[2–5] By 2030, 8.3 million population are estimated to die from tobacco consumption, accounting for up to 10% of all-cause mortality worldwide.[6] Notably, previous evidence indicated that smoking was associated with malignant HTN,[7] causing an acute rise in BP, and was the major risk factor for new-onset CVD events in patients with HTN.

In recent decades, accumulating studies have focused on the potential role of gut microbiome, which is considered as an important factor in modulating host health.[8,9] Overwhelming evidence demonstrated that current smokers possessed a distinct gut microbiome

Pan Wang and Ying Dong contributed equally to this study.

compared with never smokers, with decreased gut microbial diversity and increased abundance of *Bacteroidetes*.[10,11] Correspondingly, a profound shift in the microbial composition, including higher microbial diversity, enriched *Firmicutes* and *Actinobacteria*, as well as a lower proportion of *Bacteroidetes*, was observed following smoking cessation.[12] Thus, the alterations of the gut microbiome are presumed to be affected by the smoking status of the host.

In addition, many lines of evidence have indicated that the gut microbial community is linked to BP changes of the host. For example, investigators have revealed reduced BP by probiotic treatments in both rat models and human clinical trials of HTN.[13,14] A previous study found a dramatic decrease in microbial richness and diversity, and transformation into *Prevotella*-dominated gut enterotype in both prehypertensive and hypertensive populations. Interestingly, elevated BP was transferrable through intestinal microbiota by fecal transplantation from hypertensive human donors to germ-free mice, and the direct influence of gut microbiota (GM) on BP of the host was proved.[15]

Given emerging evidence showing the implication of smoking status in consequent GM dysbiosis and the causal role of intestinal microbiota in contributing to HTN development, the question was whether tobacco use aggravated GM dysbiosis through regulating the composition and function in patients with HTN. To address this, metagenomic sequencing of stool samples of 59 participants with and without HTN or smoking was conducted.

2 | MATERIALS AND METHODS

2.1 | Study cohort

The participants were drawn from a previous study.[15] We excluded participants with prehypertension, or no complete data on smoking in the previous study. And 59 samples were enrolled ultimately in the present study. All the participants included in the present study were strictly recruited, and none of them was under antihypertensive treatment. BP of participants was measured by nurses or physicians in a sitting position. With a random-zero mercury column sphygmomanometer, we recorded three readings at 5 min interval, and used the average of the three measurements as the final reading. HTN was defined as systolic BP (SBP) ≥140 mm Hg and/or diastolic BP (DBP) ≥90 mm Hg. Without HTN (CTR) was defined as SBP ≤125 mm Hg and DBP ≤80 mm Hg as previously described.[15] Smokers were defined as participants who ≥1 cigarette per day for more than half a year, and nonsmokers were participants who never smoked.[16] According to the status of smoking and HTN, the participants were categorized into four subgroups: nonsmokers without HTN (NS-CTR, $n = 9$), smokers without HTN (S-CTR, $n = 9$), nonsmokers with HTN (NS-HTN, $n = 18$), and smokers with HTN (S-HTN, $n = 23$).

Participants suffering from cancer, heart failure, renal failure, stroke, peripheral artery disease, and chronic inflammation were excluded. Furthermore, none of the participants took statin, aspirin, insulin, metformin, or nifedipine before sampling. Individuals who received antibiotics or probiotics treatment in the last 8 weeks were also excluded. Ethics approval was obtained from Kailuan General Hospital, Beijing, Chaoyang Hospital, and Fuwai Hospital. Written informed consent for the survey was obtained from all participants prior to data collection.

2.2 | DNA extraction and library preparation

Fecal samples were collected into a sterile container, transferred to the laboratory with ice pack and froze at −80°C until analysis. According to the manufacturer's recommendations, we extracted DNA from stool samples using TIANGEN kit. We fragmented qualified DNA by ultrasonic processor and constructed library of approximately 300 bp clone insert sizes per sample. With read length at 150 bp, paired-end sequencing was conducted by Illumina platform. The reads aligned to the human genome with Short Oligonucleotide Analysis Package 2 [SOAP2] Version 2.21, at parameters: -s 135, -l 30, -v 7, -m 200, -x 400 were removed. Remaining reads with high quality were used for further analysis.

2.3 | Metagenomic sequencing and gene catalog construction

The raw metagenomic sequencing data of 59 fecal specimens assessed in the present study were from a published study in a public database at the EMBL European Nucleotide Archive under the BioProject accession code PRJEB13870 (http://www.ebi.ac.uk/ena/data/view/PRJEB13870). Gene catalog was performed as described in a previous study.[15] Briefly, paired-end sequencing was conducted on the Illumina platform (insert size 300 bp and read length 125 bp). After quality control, the reads aligned to the human genome were removed, and the remaining high-quality reads were used for further analysis.

2.4 | Microbial diversity

The within-sample α-diversity was used to estimate the bacterial diversity of the sample based on calculating the Shannon index (richness and evenness), Chao richness, and Pielou evenness with R software (version 3.3.3, package vegan) at genus and species levels.

The β-diversity was analyzed to assess the differences in microbial communities between samples. Nonmetric dimensional scaling (NMDS), principal component analysis (PCA), and principal coordinate analysis (PCoA) were performed to determine the differences at the genus and species levels. NMDS was calculated by the vegan package, PCA by the FactoMineR package, and PCoA by the vegan and ape packages in R software (version 3.3.3). In addition, we also performed of β-diversity on axes by Kruskal-Wallis test as other investigators did previously.[17,18]

2.5 | Enterotypes

Enterotype was described as being densely populated areas in a multidimensional space of community composition.[19] In our study, enterotype was performed as previously described by Arumugam M et al.[19] Briefly, all samples were analyzed by the Partitioning Around Medoids (PAM) clustering method based on the Jensen-Shannon divergence (JSD). The optimal number of clusters was assessed using Calinski-Harabasz index.[19] Only genera with a mean relative $\geq 10^{-4}$ and presented in ≥6 samples were eligible for the final analysis. Moreover, chi-square test was used to assess the differences of enterotype distribution among four groups.

2.6 | Taxonomic annotation and abundance profiling

Genes were aligned to the integrated NR database to evaluate the taxonomic assignment using DIAMOND (version 0.7.9.58, default parameters except that −k 50 −sensitive −e 0.00001). As described in a previous study,[15] the significant matches of each gene were defined as e-values ≤10 × e-value of the top hit. These retaining matches were used to distinguish taxonomic groups. The taxonomical level of each gene was determined using the lowest common ancestor-based algorithm and processed by Metagenome Analyzer.[20] The abundance of a taxonomic group was calculated by summing the abundance of genes annotated to the same feature.

2.7 | Functional annotation

Genes were functionally annotated using DIAMOND (Version 0.7.9.58, default parameters except that −k 50 −sensitive −e 0.00001) aligned to the Kyoto Encyclopedia of Genes and Genomes (KEGG) (Release 73.1, with animal and plant genes removed) database. Each protein was assigned to the KEGG module by the highest scoring annotated hit(s) containing at least one high-scoring segment pair scoring >60 bits.[21] In addition, the abundance of the KEGG module was assessed by the total abundance of genes annotated to a feature.

2.8 | Statistical analysis

Quantitative data with nonnormal distributions were presented as median (first quartile, third quartile). Nonparametric test (Wilcoxon rank-sum test, Kruskal-Wallis test) was used for between-group comparisons. Quantitative data for α- and β-diversity and taxonomic abundance were presented as median (first quartile, third quartile). Differential abundance of genera, species, and KEGG modules was determined using the Wilcoxon rank-sum test, and the *p* values were corrected for multiple testing using the Benjamini and Hochberg method, shown as *q* values. All statistical tests were two sided, and *p* or *q* less than .05 was regarded as significant.

3 | RESULTS

3.1 | General characteristics of participants

In the present study, 9 NS-CTR, 9 S-CTR, 18 NS-HTN, and 23 S-HTN were recruited from the study cohort of a previous study.[15] The baseline characteristics of the overall study population (n = 59) and those stratified by smoking and HTN status are presented in Table 1. Compared with NS-CTR, S-CTR possessed higher hip circumference, abdominal circumference, and lower high-density lipoprotein cholesterol values. In addition, the baseline characteristics of NS-HTN and S-HTN were quite similar, except statistical differences in the serum triglyceride level.

3.2 | Gut microbial diversity between S-HTN and NS-HTN

For sequencing data production, a total of 338.74 Gb 125 bp paired-end reads were generated from raw data (371.93 Gb), with an average of 5.74 ± 0.98 (s.d.) million reads per sample (Table S1). The assembled long contigs and scaffolds from high-quality sequencing readings were applied for further gene prediction, taxonomic classification, and functional annotation.

First, the independent effect of cigarette smoking on GM diversity was assessed. The α-diversity, including Shannon, Chao, and Pielou index, and β-diversity, including NMDS, PCA, and PCoA, were calculated to evaluate the microbial diversity between nonsmokers (n = 27) and smokers (n = 32) at genus and species levels. Despite no statistically significant difference, smokers showed a decreasing tendency in the gene number and α-diversity parameters compared with the nonsmokers at the genus (p = .102 for gene number, Figure 1A; p = .3142 for Shannon index, Figure 1B; p = .3573 for Chao richness, Figure 1C; p = .2343 for Pielou evenness, Figure 1D) and species level (p = .048 for Shannon index, Figure 1E; p = .263 for Chao richness, Figure 1F; p = .079 for Pielou evenness, Figure 1G). In addition, at the genus and species levels, β-diversity, including NMDS, PCA, and PCoA, failed to distinguish participants with different smoking status (all p > .05, Figure 1H–J,k–M).

Hypertension was taken into account to evaluate the role of smoking in aggravating GM dysbiosis in individuals with HTN. The participants were divided into 4 groups: 9 NS-CTR, 9 S-CTR, 18 NS-HTN, and 23 S-HTN. Compared with NS-HTN or S-CTR, the α-diversity parameters were lower (marginal significant) in S-HTN (p = .0956 for Shannon index, Figure 2B; p = .0903 for Pielou evenness, Figure 2D for NS-HTN vs. S-HTN; p = .0583 for Shannon index, Figure 2C; p = .0858 for Pielou evenness, Figure 2D for S-CTR vs. S-HTN) at genus level. Furthermore, at the level of species, we found that no significant difference among the four groups (Shannon index, Figure 2E; Chao richness, Figure 2F and Pielou evenness, Figure 2G. all p > .05). In addition, β-diversity in NMDS, PCA, and PCoA plots at the genus and species levels were also assessed. For the genus level (Figure 2H–J) and species level (Figure 2K–M), NMDS, PCA, and

TABLE 1 General characteristics of study participants

Characteristics	NS-CTR	S-CTR	NS-HTN	S-HTN	p_1 value	p_2 value
Number	9	9	18	23		
Age (year)	56.00 (46.50–59.00)	57.00 (54.00–62.00)	56.50 (50.75–59.25)	51.00 (47.00–58.00)	.25	.09
Male/female	9 (5/4)	9 (9/0)	18 (16/2)	23 (23/0)	.08	.19
Smoking history						
Smoking duration (year)	0.00	35.00 (30.00–40.00)	0.00	25.00 (20.00–35.00)	<.01*	<.01*
Smoking amount (cigarette/day)	0.00	20.00 (10.00–22.50)	0.00	20.00 (10.00–30.00)	<.01*	<.01*
Smoking coefficient (year cigarette/day)	0.00	525.00 (400.00–730.00)	0.00	500.00 (280.00–760.00)	<.01*	<.01*
SBP	115.00 (108.00–118.17)	115.33 (107.33–121.50)	147.50 (142.92–153.08)	147.33 (139.67–156.67)	.63	.49
DBP	71.67 (64.84–76.84)	72.00 (70.00–77.00)	93.00 (88.75–98.00)	93.00 (90.00–100.00)	.79	.44
HR	71.00 (67.50–76.00)	67.00 (63.00–79.50)	72.50 (67.00–79.25)	71.00 (65.00–77.00)	.45	.39
Body mass index	23.88 (20.64–24.84)	24.91 (21.66–25.46)	25.10 (23.51–26.48)	26.17 (24.93–27.78)	.40	.16
WAIST_C	80.00 (74.50–89.50)	88.00 (85.00–100.00)	86.00 (83.00–97.75)	90.00 (84.50–100.00)	.08	.43
HIP_C	92.50 (87.25-100.75)	100.00 (95.50–112.00)	100.50 (91.50–110.00)	105.00 (94.25–108.50)	.03*	.40
ABDOM_C	82.00 (76.25–93.50)	93.00 (90.00–105.00)	90.50 (86.50–98.75)	95.00 (88.00–105.00)	.02*	.27
Uric acid	294.00(124.50–317.00)	330.00 (289.50–360.50)	403.58 (311.50–445.00)	374.00 (331.00–414.00)	.27	.63
Creatinine	77.00 (60.50–176.70)	87.00 (72.00–97.85)	71.50 (58.00–100.60)	73.00 (65.00–95.00)	.69	.50
Fasting blood glucose	5.25 (4.80–5.60)	5.15 (4. 70–5.32)	5.54 (5.11–6.25)	5.58 (5.28–6.18)	.57	.71
Total cholesterol	5.30 (4.65–6.07)	5.77 (4.48–6.40)	5.60 (4.89–6.46)	5.86 (5.16–6.79)	.63	.26
Triglyceride	0.92 (0.77–1.36)	0.96 (0.69–2.43)	1.20 (0.70–2.17)	2.04 (1.14–3.07)	.66	.03*
High-density lipoprotein	1.53 (1.26–1.58)	1.14 (0.90–1.26)	1.32 (1.20–1.74)	1.28 (1.05–1.54)	.03*	.28
Low-density lipoprotein	2.83 (2.06–3.29)	2.84 (2.61–3.35)	2.84 (2.29–3.45)	2.78 (2.15–3.36)	.57	.93
Total protein	74.00 (68.00–78.45)	75.00 (70.75–80.90)	74.00 (72.00–77.78)	75.60 (72.00–77.00)	.74	.78
Hemoglobin	145.00 (128.00–165.00)	159.60 (136.00–165.00)	156.00 (151.00–161.50)	161.00 (155.00–167.00)	.06	.11
White blood cell	5.90 (5.30–7.10)	6.30 (5.09–8.32)	6.55 (5.33–7.60)	6.20 (5.50–7.10)	.90	.67

Note: P_1 value: NS-CTR versus S-CTR P_2 value: NS-HTN versus S-HTN. *$p < .05$.

Abbreviations: ABDOM_C, abdominal circumference; HIP_C, hip circumference; NS-CTR, nonsmokers without HTN; NS-HTN, nonsmokers with HTN; S-CTR, smokers without HTN; S-HTN, smokers with HTN; WAIST_C, waist circumference.

FIGURE 1 Alterations of gut microbial diversity in individuals from the smoking (S, $n = 32$) group compared with the Nonsmoking (NS, $n = 27$) group. (A–D) Gene number and α-diversity indexes, including Shannon index, Chao richness, and Pielou evenness, based on the genus profiles in NS and S cohort ($p = .1022$ for gene number; $p = .3142$ for Shannon index; $p = .3573$ for Chao richness; $p = .2343$ for Pielou evenness, respectively; Kruskal-Wallis test). (E–G) α-diversity indexes, including Shannon index, Chao richness, and Pielou evenness, based on the species profiles in NS and S cohort ($p = .0483$ for Shannon index; $p = .2634$ for Chao richness; $p = .0788$ for Pielou evenness, respectively; Kruskal-Wallis test). Boxes represent the interquartile ranges, the inside line or points represent the median, and circles are outliers. Blue, NS group; Purple, S group. (H–J) β-Diversity including NMDS, PCA, and PCoA of NS and S participants based on the genus profiles. (K–M) NMDS, PCA, and PCoA of the NS and S groups were performed at the species level, respectively. Circles in blue indicate samples from the NS group, and triangles in purple indicate individuals from the S group

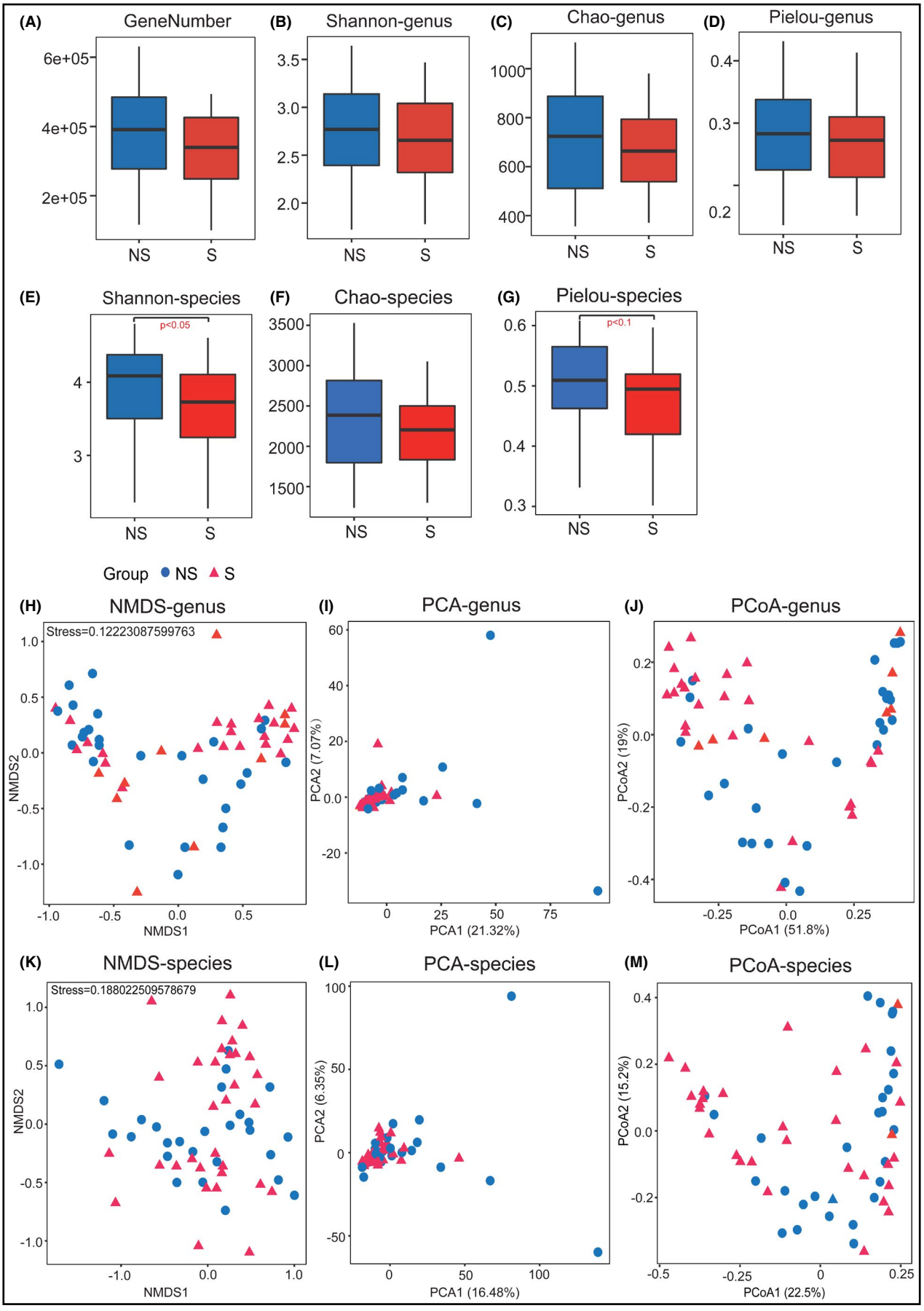
(A)
GeneNumber
6e+05
4e+05
2e+05
NS
S
(B)
Shannon-genus
3.5
3.0
2.5
2.0
NS
S
(C)
Chao-genus
1000
800
600
400
NS
S
(D)
Pielou-genus
0.4
0.3
0.2
NS
S
(E)
Shannon-species
p<0.05
4
3
NS
S
(F)
Chao-species
3500
3000
2500
2000
1500
NS
S
(G)
Pielou-species
p<0.1
0.6
0.5
0.4
0.3
NS
S
Group NS S
(H)
NMDS-genus
Stress=0.12223087599763
NMDS2
NMDS1
(I)
PCA-genus
PCA2 (7.07%)
PCA1 (21.32%)
(J)
PCoA-genus
PCoA2 (19%)
PCoA1 (51.8%)
(K)
NMDS-species
Stress=0.188022509578679
NMDS2
NMDS1
(L)
PCA-species
PCA2 (6.35%)
PCA1 (16.48%)
(M)
PCoA-species
PCoA2 (15.2%)
PCoA1 (22.5%)

PCoA analysis failed to cluster participants into different groups. *p* values derived from PERMANOVA Adonis test of any difference by categories were >.05 for PCA at genus and species levels (Figure 2H–M). Moreover, we also performed analysis on β-diversity on axes. And we found evidence that the second NMDS (P_{NMDS2} = 0.008, Figure 2H) and second PCoA (P_{PCoA2} = 0.010, Figure 2J) differed significantly between S-HTN and S-CTR at genus level. In addition, we found that the first PCA (P_{PCA1} = 0.038, Figure 2L) and second PCoA (P_{PCoA2} = 0.004, Figure 2M) showed difference between S-HTN and S-CTR at the species level. The biological meaning of such statistical different at one axis of NMDS, PCA, or PCoA suggests a difference of β-diversity to some extent on another side.

3.3 | Enterotype distribution indicated an inclination to Prevotella-dominated type in S-HTN

The microbial enterotype features were analyzed by PAM clustering method based on JSD to explore the global differences in the gut microbiome community structures in the cohort. The 59 samples were clustered into 2 enterotypes by the PCA of JSD values at the genus level (Figure 3A). *Prevotella* and *Bacteroides* were found to be the most enriched genera in each enterotype, respectively (*p* = 2.02e−16 and *p* = 1.02e−08, respectively, Figure 3B,C). In addition, the percentage and number of subjects distributed in enterotypes *Prevotella* and *Bacteroides* were examined. Compared with the other three groups, S-HTN exhibited a higher percentage in enterotype *Prevotella*, but lower percentage distributed in enterotype *Bacteroides*. Moreover, 69.57% (*n* = 16) S-HTN exhibited enterotype *Prevotella* and 30.43% (*n* = 7) exhibited enterotype *Bacteroides*. However, only 33.33% (*n* = 3) of the populations in NS-CTR, 55.56% (*n* = 5) in S-CTR, and 50.00% (*n* = 9) in NS-HTN were assigned into enterotype *Prevotella* (Figure 3D,E), although no statistical difference was found (chi-square=3.857, *p* = .277). These findings suggested that enterotype was inclined to *Prevotella*-dominated type in S-HTN.

3.4 | Smokers with HTN disease showed dramatic changes in intestinal genera and species composition

Taxonomic annotation and abundance profiles were analyzed to assess alterations in the microbial composition among groups (Figure 4). Overall, the participants shared 1126 genera and 3752 species (Figure 4A,D). The top 10 most abundant genera, such as *Prevotella*, *Bacteroides*, and *Faecalibacterium*, and the top 10 species, such as *Faecalibacterium prausnitzii*, *P copri*, and *Pcopri* CAG:164, were detected (Figure 4B,E). In addition, the relative abundance of the top 10 genera and species in each participant from different profiles of smoking and HTN was also assessed (Figure 4C,F). Compared with NS-CTR, S-CTR and NS-HTN showed a higher abundance of genera *Prevotella* and *Faecalibacterium* (Figure 4B,C) and species *Sutterella wadsworthensis* (Figure 4E,F).

Given the difference in gut microbial diversity and structure among groups, the microbes dramatically and differently enriched at the genus and species levels were analyzed (q < 0.05, the *p* values were assessed using Wilcoxon rank-sum test and corrected for multiple testing by the Benjamin and Hochberg method). In order to show it clear, the relative abundance of genera, species level has been transformed into log 10 values. Compared with S-CTR, bacteria of 168 (128 specific +40 shared) genera (Figure 5A and Table S2) and 472 (349 specific +123 shared) species (Figure 6A and Table S3) were statistically different in S-HTN, which might be associated with HTN in smokers. Compared with NS-HTN, 119 (79 specific +40 shared) genera (Figure 5A) and 384 (261 specific +123 shared) species (Figure 6A) were observed to be significantly different in S-HTN, which might be potential GM in HTN development linked to smoking status. Above all, the different common bacteria obtained from the overlap between S-CTR versus S-HTN and NS-HTN versus S-HTN were mostly HTN-related bacteria, including 40 genera and 123 species, which might be altered by the smoking status (Figure 5A and Figure 6A).

Then, the abundance of the top 15 of the 40 shared differential genera, such as *Oribacterium, Atopobium*, and *Peptoniphilus*, are shown in Figure 5B, and the top 15 of 123 shared differential species, such as *Anaerotruncus colihominis*, *Clostridium asparagiforme*, and *Eubacterium plexicaudatum*, are further clustered in Figure 6B. It was quite absorbing that these different genera and species ultimately exhibited a deficiency in S-HTN compared with simple smokers and nonsmokers with HTN, indicating GM dysbiosis. Moreover, the relative abundance of the top 15 common differential genera (Figure 5C) and species (Figure 6C) in each group were assessed. The relative abundance had a decreasing tendency from NS-CTR, S-CTR, and NS-HTN to S-HTN, such as *Phycisphaera* at the genus level and *Clostridium asparagiforme* at the species level. Importantly, the relative abundance of these intestinal bacteria was found to be

FIGURE 2 Shifts of intestinal microbiota in α- and β-diversity between NS-HTN and S-HTN. (A–D) Box plots show gene number, Shannon index, Chao richness, and Pielou evenness at the genus level in each group. (E–G) Box plots show Shannon index, Chao richness, and Pielou evenness at species level in each group. CTR, nonhypertensive controls; HTN, patients with HTN; NS, nonsmokers; and S, smokers. Green, NS-CTR, *n* = 9; cyan, S-CTR, *n* = 9; yellow, NS-HTN, *n* = 18; orange, S-HTN, *n* = 23. (H–J) NMDS, PCA, and PCoA plots based on the genera level in groups. Significant differences across groups were established at NMDS2, PCA1, and PCoA2 at genus level. Circles in green indicate samples from the NS-CTR group, circles in cyan indicate samples from the S-CTR group, triangles in yellow indicate individuals from the NS-HTN group, and triangles in orange indicate individuals from S-HTN group. (K–M) Scatter diagram showing the NMDS, PCA, and PCoA plots at the species level. Significant differences across groups were established at PCA1, and PCoA2 at species level between S-CTR and S-HTN. Boxes represent the interquartile ranges, the inside line or points represent the median, and circles represent outliers. $^{*}p < .05$; $^{\#}p < .1$; Kruskal-Wallis test

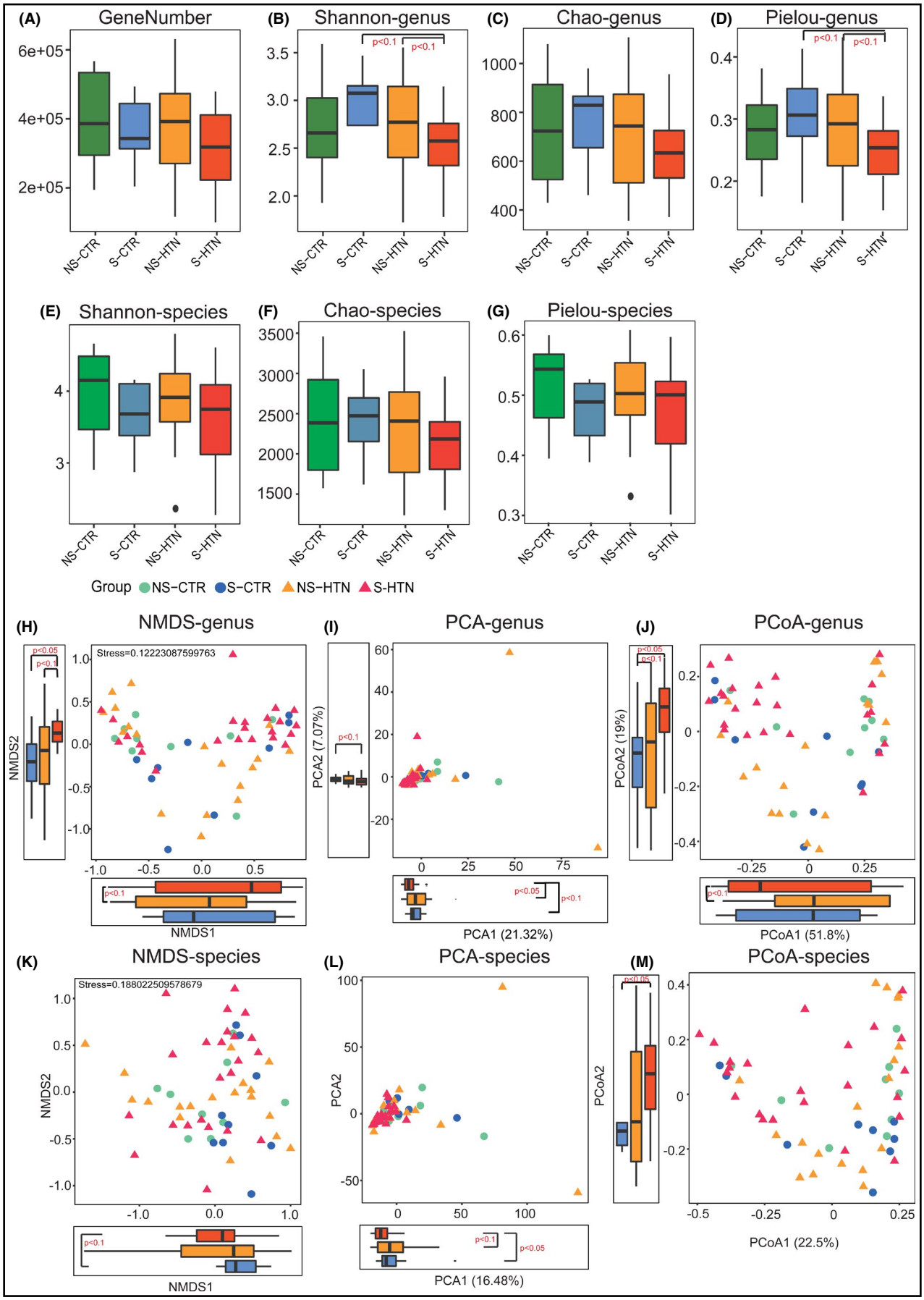
(A) GeneNumber
(B) Shannon-genus
(C) Chao-genus
(D) Pielou-genus
(E) Shannon-species
(F) Chao-species
(G) Pielou-species
NS-CTR
S-CTR
NS-HTN
S-HTN
p<0.1
Group NS-CTR S-CTR NS-HTN S-HTN
(H) NMDS-genus
Stress=0.12223087599763
NMDS1
NMDS2
(I) PCA-genus
PCA1 (21.32%)
PCA2 (7.07%)
p<0.05
(J) PCoA-genus
PCoA1 (51.8%)
PCoA2 (19%)
(K) NMDS-species
Stress=0.188022509578679
(L) PCA-species
PCA1 (16.48%)
PCA2
(M) PCoA-species
PCoA1 (22.5%)
PCoA2

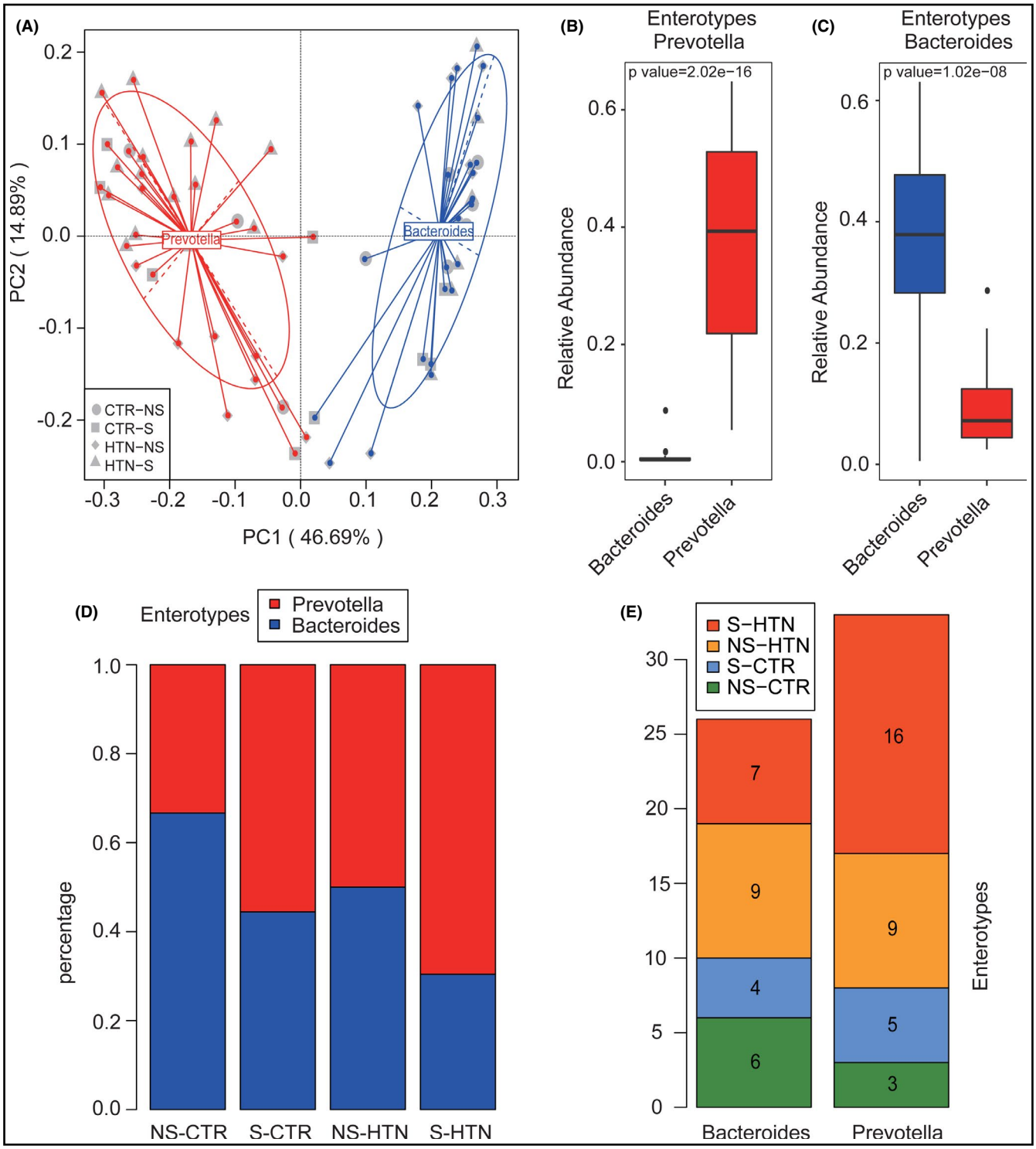

FIGURE 3 Altered distributions in gut enterotypes of S-HTN and NS-HTN. (A) A total of 59 samples in the study cohort were clustered into enterotype 1 (red) and enterotype 2 (blue) by PCA of JSD values at the genus level. The top contributors in the two enterotypes were *Prevotella* and *Bacteroides*, respectively. (B and C) The relative abundance of *Prevotella* and *Bacteroides* in enterotype 1 and enterotype 2; p = 2.02e−16 and p = 1.02e−08, respectively; Wilcoxon rank-sum test. (D and E) The percentage and number of samples in each group distributed in enterotype 1 and enterotype 2. Boxes represent the interquartile ranges, the inside line or points represent the median, and circles are outliers. Chi-square = 3.857, p = .277

FIGURE 4 Genera and species annotated in the gut of S-HTN and NS-HTN. (A and D) Venn diagrams showing the number of genera and species annotated in groups. A total of 1126 genera and 3752 species shared in NS-CTR, S-CTR, NS-HTN, and S-HTN groups. (B and E) Bar plots showing the relative abundance of the top 10 genera and species in each group. Different genera and species are differentiated by color. (C and F) The relative abundance of the top 10 genera and species in each participant from different groups

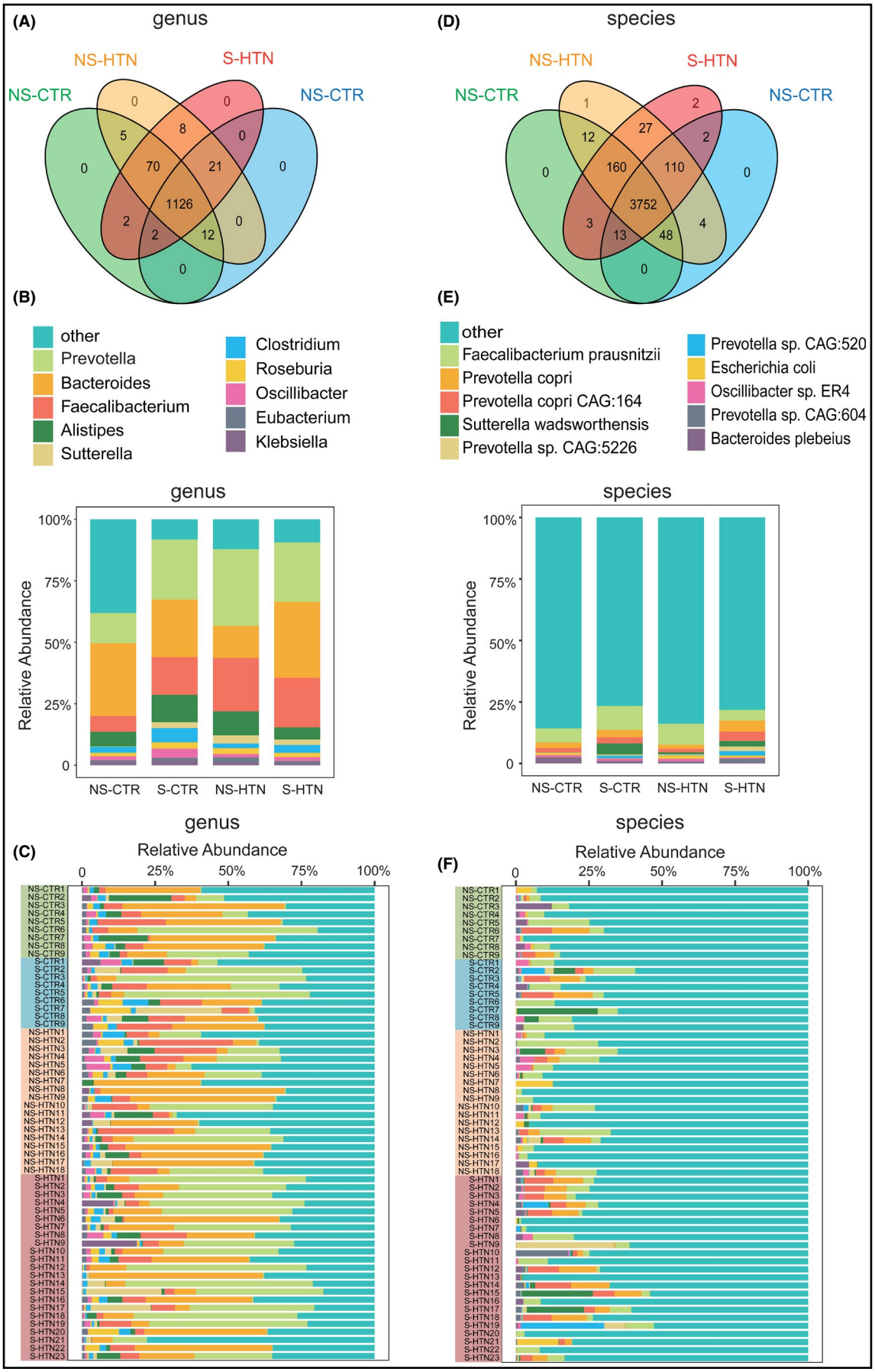
(A)
genus
NS-HTN
S-HTN
NS-CTR
NS-CTR
0
0
5
8
0
0
70
21
0
1126
2
0
2
12
0
(D)
species
NS-HTN
S-HTN
NS-CTR
NS-CTR
1
2
12
27
2
160
110
0
3752
3
4
13
48
0
(B)
other
Prevotella
Bacteroides
Faecalibacterium
Alistipes
Sutterella
Clostridium
Roseburia
Oscillibacter
Eubacterium
Klebsiella
(E)
other
Faecalibacterium prausnitzii
Prevotella copri
Prevotella copri CAG:164
Sutterella wadsworthensis
Prevotella sp. CAG:5226
Prevotella sp. CAG:520
Escherichia coli
Oscillibacter sp. ER4
Prevotella sp. CAG:604
Bacteroides plebeius
genus
Relative Abundance
100%
75%
50%
25%
0
NS-CTR
S-CTR
NS-HTN
S-HTN
species
Relative Abundance
100%
75%
50%
25%
0
NS-CTR
S-CTR
NS-HTN
S-HTN
(C)
genus
Relative Abundance
0
25%
50%
75%
100%
NS-CTR1
NS-CTR2
NS-CTR3
NS-CTR4
NS-CTR5
NS-CTR6
NS-CTR7
NS-CTR8
NS-CTR9
S-CTR1
S-CTR2
S-CTR3
S-CTR4
S-CTR5
S-CTR6
S-CTR7
S-CTR8
S-CTR9
NS-HTN1
NS-HTN2
NS-HTN3
NS-HTN4
NS-HTN5
NS-HTN6
NS-HTN7
NS-HTN8
NS-HTN9
NS-HTN10
NS-HTN11
NS-HTN12
NS-HTN13
NS-HTN14
NS-HTN15
NS-HTN16
NS-HTN17
NS-HTN18
S-HTN1
S-HTN2
S-HTN3
S-HTN4
S-HTN5
S-HTN6
S-HTN7
S-HTN8
S-HTN9
S-HTN10
S-HTN11
S-HTN12
S-HTN13
S-HTN14
S-HTN15
S-HTN16
S-HTN17
S-HTN18
S-HTN19
S-HTN20
S-HTN21
S-HTN22
S-HTN23
(F)
species
Relative Abundance
0
25%
50%
75%
100%
NS-CTR1
NS-CTR2
NS-CTR3
NS-CTR4
NS-CTR5
NS-CTR6
NS-CTR7
NS-CTR8
NS-CTR9
S-CTR1
S-CTR2
S-CTR3
S-CTR4
S-CTR5
S-CTR6
S-CTR7
S-CTR8
S-CTR9
NS-HTN1
NS-HTN2
NS-HTN3
NS-HTN4
NS-HTN5
NS-HTN6
NS-HTN7
NS-HTN8
NS-HTN9
NS-HTN10
NS-HTN11
NS-HTN12
NS-HTN13
NS-HTN14
NS-HTN15
NS-HTN16
NS-HTN17
NS-HTN18
S-HTN1
S-HTN2
S-HTN3
S-HTN4
S-HTN5
S-HTN6
S-HTN7
S-HTN8
S-HTN9
S-HTN10
S-HTN11
S-HTN12
S-HTN13
S-HTN14
S-HTN15
S-HTN16
S-HTN17
S-HTN18
S-HTN19
S-HTN20
S-HTN21
S-HTN22
S-HTN23

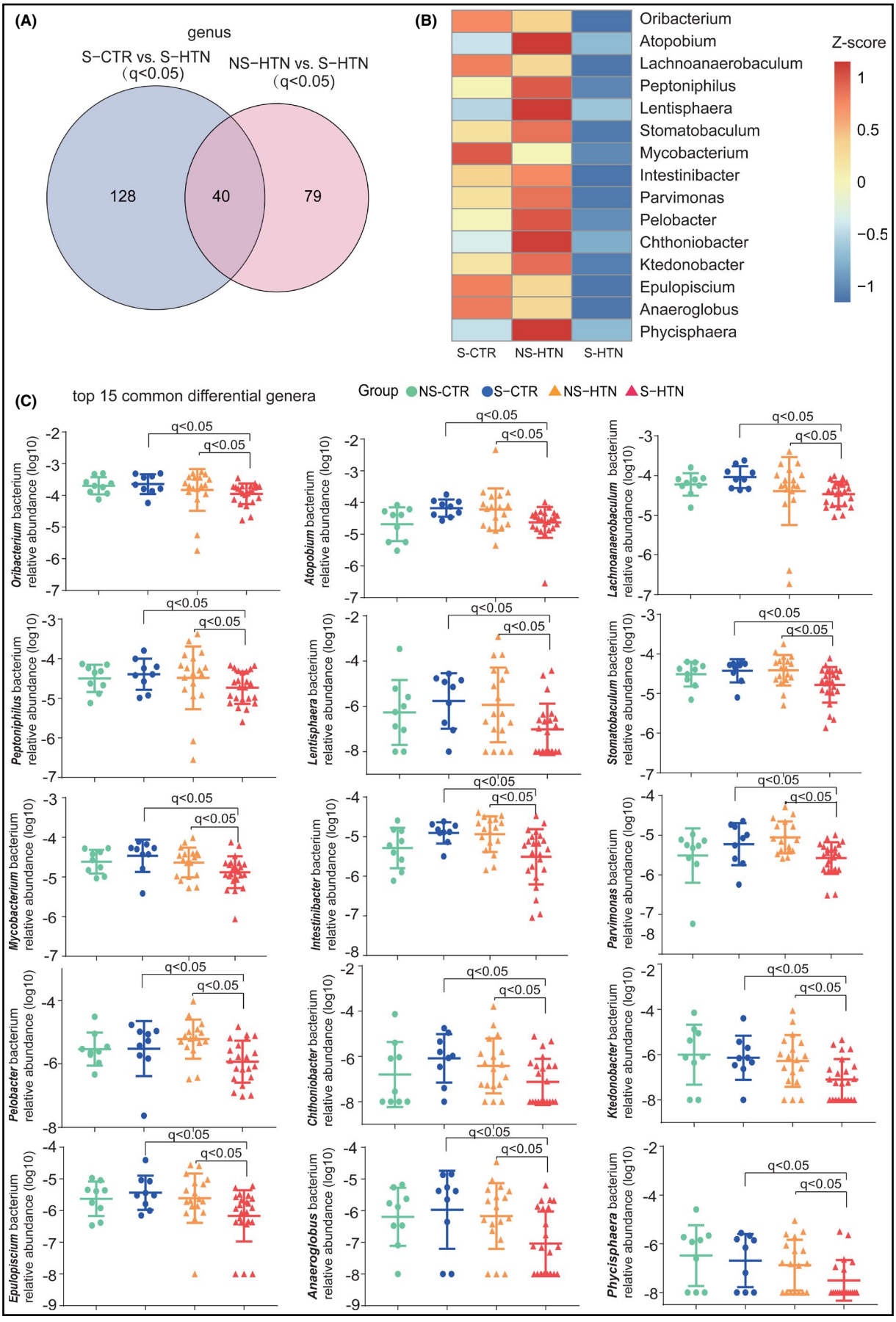
(A)
genus
S−CTR vs. S−HTN (q<0.05)
NS−HTN vs. S−HTN (q<0.05)
128
40
79
(B)
Oribacterium
Atopobium
Lachnoanaerobaculum
Peptoniphilus
Lentisphaera
Stomatobaculum
Mycobacterium
Intestinibacter
Parvimonas
Pelobacter
Chthoniobacter
Ktedonobacter
Epulopiscium
Anaeroglobus
Phycisphaera
S-CTR
NS-HTN
S-HTN
Z-score
1
0.5
0
−0.5
−1
(C)
top 15 common differential genera
Group NS-CTR S-CTR NS-HTN S-HTN
q<0.05
Oribacterium bacterium relative abundance (log10)
Atopobium bacterium relative abundance (log10)
Lachnoanaerobaculum bacterium relative abundance (log10)
Peptoniphilus bacterium relative abundance (log10)
Lentisphaera bacterium relative abundance (log10)
Stomatobaculum bacterium relative abundance (log10)
Mycobacterium bacterium relative abundance (log10)
Intestinibacter bacterium relative abundance (log10)
Parvimonas bacterium relative abundance (log10)
Pelobacter bacterium relative abundance (log10)
Chthoniobacter bacterium relative abundance (log10)
Ktedonobacter bacterium relative abundance (log10)
Epulopiscium bacterium relative abundance (log10)
Anaeroglobus bacterium relative abundance (log10)
Phycisphaera bacterium relative abundance (log10)

FIGURE 5 Genera significantly different between S-HTN and S-CTR, and between S-HTN and NS-HTN. (A) Venn diagrams demonstrating the number of differential genera when comparing S-CTR and S-HTN, and NS-HTN and S-HTN. The overlap identified 40 genera concurrently altered; $q < 0.05$, Wilcoxon rank-sum test. (B) Heat map showing the top 15 of the 40 shared differential genera in S-CTR, NS-HTN, and S-HTN. The abundance profiles were expressed by *Z* scores, and genera were clustered based on Bray-Curtis distance in the clustering tree. The *Z* score was negative (shown in blue) when the row abundance was lower than the mean, and was shown in red when the row abundance was higher than the mean. (C) Scatter plots of relative abundance of the top 15 shared differential genera shared between S-HTN vs. S-CTR, and S-HTN vs. NS-HTN. In order to show it clear, the relative abundance of genera level has been transformed into log10 values. Green, NS-CTR; cyan, S-CTR; yellow, NS-HTN; and orange, S-HTN. The dots indicate individual values of the participants, and the horizontal lines from bottom to top represent 25th percentiles, medians, and 75th percentiles, respectively

the lowest in S-HTN, regardless of the genus or species level. It was thus speculated that a significant decrease in these bacteria might account for the dysbiotic GM of HTN caused by smoking.

3.5 | Intestinal function alteration of S-HTN

The KEGG database was used to annotate the gut microbial gene functions across groups in the present study cohort. First of all, 31 (21 specific +10 shared) differential KEGG modules existed between S-CTR and S-HTN, which separated S-HTN from S-CTR. Moreover, 48 (38 specific +10 shared) different KEGG modules existed between NS-HTN and S-HTN, which were functions related to the smoking status. The overlap identified that 10 KEGG modules were shared, which were not only attributed to the smoking status but also associated with HTN (Figure 7A and Table S4). The 10 shared KEGG modules differently enriched in S-CTR, NS-HTN, and S-HTN are shown in Figure 7B. Consistent with the observations in microbial profiles at the genus and species levels, these KEGG functional modules displayed a significant reduction in S-HTN. Further analysis based on NMDS, PCA, and PCoA of the KEGG modules showed that compared with NS-HTN or S-CTR, the alteration of GM function in S-HTN was discrepant ($P_{\text{NMDS S-CTR vs. S-HTN}} = 0.0216$, $P_{\text{NMDS NS-HTN vs. S-HTN}} = 0.0357$; $P_{\text{PCA S-CTR vs. S-HTN}} = 0.0307$, $P_{\text{PCA NS-HTN vs. S-HTN}} = 0.0219$; $P_{\text{PcoA S-CTR vs. S-HTN}} = 0.0149$, $P_{\text{PcoA NS-HTN vs. S-HTN}} = 0.0382$) (Figure 7C–E).

The functional features of the gut microbiome were dysbiotic in S-HTN, illustrating the profound impact of smoking status on GM in hypertensive individuals. The relative abundance of the 10 shared differential KEGG modules is further shown in Figure 7F. In order to show it clear, the relative abundance of KEGG modules has been transformed into log10 values. These 10 KEGG modules were found to be important in human anabolism and homeostasis. For example, the functional module M00089 was involved in triglyceride metabolism, the module M00122 was implicated in vitamin B12 metabolism, and the module M00175 functioned in nitrogen synthesis. In addition, functional modules were involved in n-acetyl carboxyl conversion into amino acids (basic amino acid synthesis, M00201), leucine biosynthesis (M00432), nucleoside biosynthesis (M00554), and galactose degradation (M00632). These observations suggested that the altered physiological and metabolic functions of GM following smoking might participate in the process of disease including HTN.

4 | DISCUSSION

In the present study, cigarette smoking was found to lead to the gut microbiome disorders in patients with HTN. Compared with smoking or hypertensive participants alternatively, the microbial α-diversity parameters were lower in participants with both smoking status and HTN, and significant differences of β-diversity axes as compared to S-CTR at genus and species level. For the bacterial features in enterotype distribution, the results suggested that compared with controls, the enterotype of GM in patients with smoking or HTN was inclined to *Prevotella*-dominant type. Importantly, S-HTN had the highest percentage distributed in enterotype *Prevotella*. Moreover, the taxa composition and potential metabolic functions of intestinal microbes in S-HTN shifted, with deficiencies of various bacterial genera, species, and functions.

In recent years, emerging evidence suggested that changes in the composition of GM were significant in CVDs and metabolic disorders, such as obesity, diabetes mellitus, and metabolic syndrome.[22-24] HTN is known as the most common modifiable risk factor for CVD. Previous studies confirmed a causal role of aberrant GM in contributing to the pathogenesis of HTN.[15] The decreased bacterial diversity, altered enterotype distribution trend to *Prevotella*, and variation in bacterial populations and their corresponding functions were identified in both prehypertensive and hypertensive adults, which were considered as dysbiotic GM in patients with HTN. Simultaneously, previous studies found that cigarette smoking, a widely known risk factor for HTN and CVD events, reduced GM diversity but also altered the composition and functional features. Thus, the findings of the present study further extended previous cognition on the relationship between smoking status, HTN, and intestinal microbiome by revealing the GM dysbiosis in a cohort with HTN following cigarette smoking.

Indeed, for intestinal microbiota of smokers, previous investigators have demonstrated significantly reduced Shannon diversity and increased abundance of *Bacteroidetes* as compared with nonsmokers.[10,11] Here we found current smokers showed a decreasing tendency with statistically significant difference at Shannon index but not the other α-diversity parameters as compared to nonsmokers at the species level. These results were consistent with previous findings from other researchers and validated the alterations of gut microbiota by tobacco smoking.

Moreover, enterotype distribution indicated an inclination to *Prevotella*-dominated type in S-HTN, but slightly lower percentage

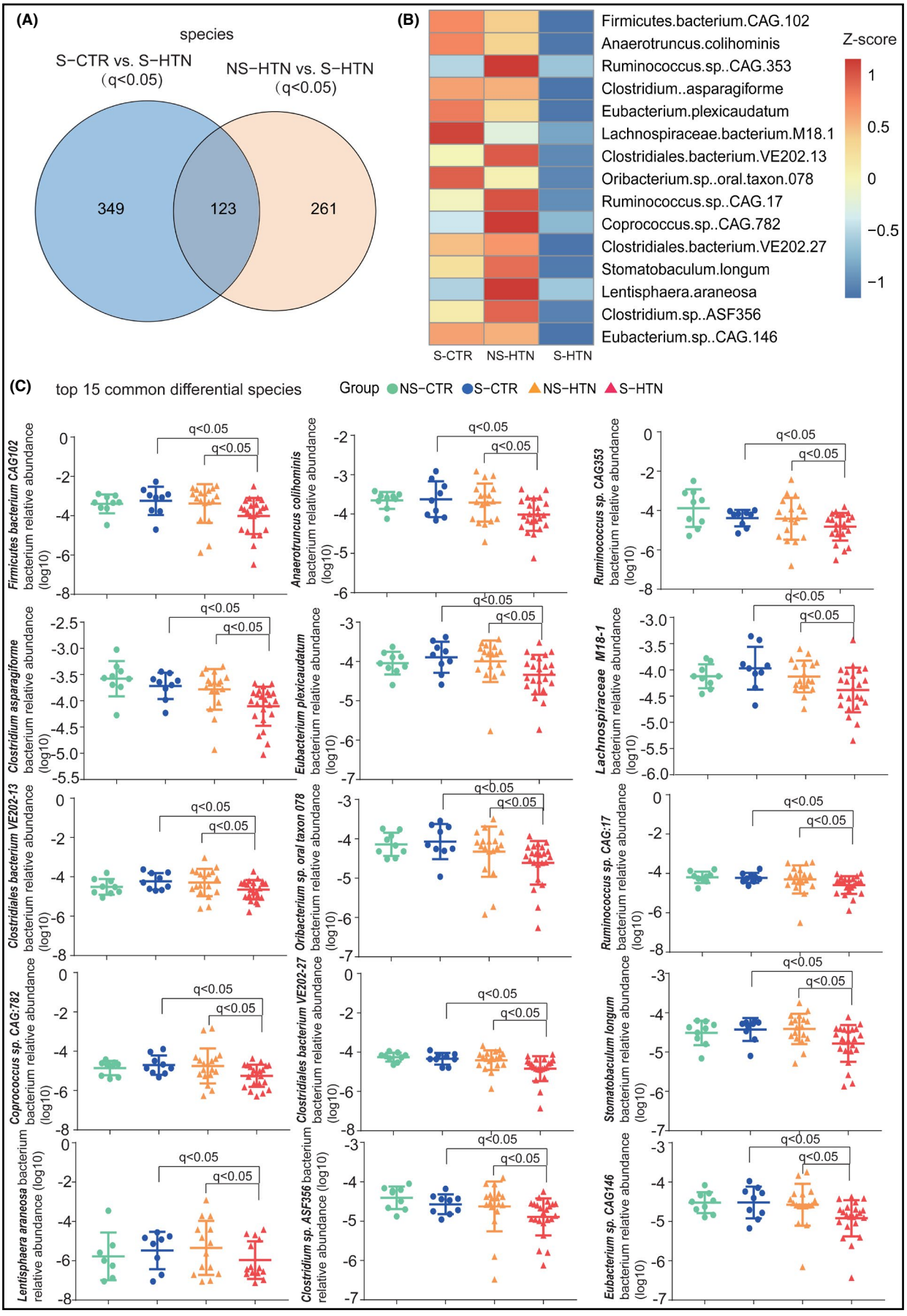
(A)
species
S−CTR vs. S−HTN (q<0.05)
NS−HTN vs. S−HTN (q<0.05)
349
123
261
(B)
Firmicutes.bacterium.CAG.102
Anaerotruncus.colihominis
Ruminococcus.sp..CAG.353
Clostridium..asparagiforme
Eubacterium.plexicaudatum
Lachnospiraceae.bacterium.M18.1
Clostridiales.bacterium.VE202.13
Oribacterium.sp..oral.taxon.078
Ruminococcus.sp..CAG.17
Coprococcus.sp..CAG.782
Clostridiales.bacterium.VE202.27
Stomatobaculum.longum
Lentisphaera.araneosa
Clostridium.sp..ASF356
Eubacterium.sp..CAG.146
S-CTR NS-HTN S-HTN
Z-score
1
0.5
0
−0.5
−1
(C)
top 15 common differential species
Group NS−CTR S−CTR NS−HTN S−HTN
Firmicutes bacterium CAG102 bacterium relative abundance (log10)
Anaerotruncus colihominis bacterium relative abundance (log10)
Ruminococcus sp. CAG353 bacterium relative abundance (log10)
Clostridium asparagiforme bacterium relative abundance (log10)
Eubacterium plexicaudatum bacterium relative abundance (log10)
Lachnospiraceae M18-1 bacterium relative abundance (log10)
Clostridiales bacterium VE202-13 bacterium relative abundance (log10)
Oribacterium sp. oral taxon 078 bacterium relative abundance (log10)
Ruminococcus sp. CAG:17 bacterium relative abundance (log10)
Coprococcus sp. CAG:782 bacterium relative abundance (log10)
Clostridiales bacterium VE202-27 bacterium relative abundance (log10)
Stomatobaculum longum bacterium relative abundance (log10)
Lentisphaera araneosa bacterium relative abundance (log10)
Clostridium sp. ASF356 bacterium relative abundance (log10)
Eubacterium sp. CAG146 bacterium relative abundance (log10)
q<0.05

FIGURE 6 Species significantly different between S-HTN and S-CTR, and between S-HTN and NS-HTN. (A) Venn diagrams demonstrating the number of differential species on comparing S-CTR and S-HTN, and between NS-HTN and S-HTN. The overlap identified 123 genera concurrently altered; $q < 0.05$, Wilcoxon rank-sum test. (B) Heat map showing the top 15 of the 123 shared differential species in S-CTR, NS-HTN, and S-HTN. The abundance profiles were expressed by *Z* scores, and the genera were clustered based on the Bray-Curtis distance in the clustering tree. The *Z* score was negative (shown in blue) when the row abundance was lower than the mean, and was shown in red when the row abundance was higher than the mean. (C) Scatter plots of the relative abundance of the top 15 shared differential species shared between S-HTN vs. S-CTR, and S-HTN vs. NS-HTN. In order to show it clear, the relative abundance of species level has been transformed into log10 values. Green, NS-CTR; cyan, S-CTR; yellow, NS-HTN; and orange, S-HTN. The dots indicate individual values of the participants, and the horizontal lines from the bottom to top represent 25th percentiles, medians, and 75th percentiles, respectively

distributed in enterotype *Bacteroides*. *Prevotella* and *Bacteroides* might have important effects on the health status and disease, among which several species of *Bacteroides* were considered to be beneficial or probiotic.[25,26] Available evidence suggested a decrease in the abundance of *Bacteroides* associated with intestinal inflammation, such as Crohn's disease.[27] In addition, reduced *Bacteroides* was also observed in obese humans[28] and mice.[29,30] On the contrary, an increased abundance of *Prevotella* in the intestine was positively associated with colon cancer[31,32] and susceptibility to colitis.[33,34] For tobacco smokers, the association was found in the gut microbiome, with an enhanced relative abundance of *Prevotella* and suppressed *Bacteroides*,[11] which deteriorated according to the findings in S-HTN. Kelly et al[35] found that Bacteroidetes was associated with low CVD risk, while *Prevotella* was related to high CVD risk. However, Boursier et al[36] found that *Bacteroidetes* was significantly increased in non-alcoholic steatohepatitis and patients with significant fibrosis, whereas *Prevotella* decreased. Thus, the roles of *Prevotella* and *Bacteroidetes* in health are still unclear and full of conflicts. The detailed functions of *Prevotella* and *Bacteroidetes* in human health and disease development still need further investigation.

For significantly different bacteria across the four groups, the overlapped bacteria we ultimately focused on were found to be the most disease-related bacteria, with both smoking and HTN. The relative abundance of the overlapping bacteria had a certain tendency among the four groups, such as *Phycisphaera* at the genus level and *Clostridium asparagiforme* at the species level, both showing a decreasing tendency from NS-CTR, S-CTR, and NS-HTN to S-HTN. Although the role of *Phycisphaera* in humans and animals has not been reported yet, a bacterial community analysis showed that *Rhodospirillales*, *Phycisphaerae*, *Chlorobiales*, and *Burkholderiales* could decompose and reduce the concentration of nitrate, nitrite, and ammonium, respectively.[37] *C asparagiforme* is known to produce acetic acid, lactic acid, and ethanol as the main products of glucose fermentation. A latest study found that supplementation with a high dose of probiotics in the drinking water significantly increased the abundance of *C asparagiforme*, *C hathewayi*, and *C saccharolyticum*, which produced butyrate and other organic acids beneficial for the maintenance of host health.[38] As the enrichment of genus *Phycisphaera* and species *C asparagiforme* decreased gradually in the four groups from NS-CTR, S-CTR, and NS-HTN to S-HTN, it was speculated that the significant decrease in the abundance of these bacteria might be involved in the pathological gut microbiome of HTN caused by smoking.

An imbalance in the gene function of bacteria was found, accompanied by the altered composition of intestinal microbiota. The functional modules involved in triglyceride metabolism, vitamin metabolism, basic amino acid synthesis, leucine biosynthesis, nucleoside biosynthesis, galactose degradation, and so on, shifted most sharply in participants with both smoking and HTN compared with participants who either smoked or were hypertensive. Most of these impaired microbial functions in S-HTN are known to be essential for health. Evidence has shown the physiological significance of vitamin metabolism pathways in host homeostasis, such as maintaining plasma prothrombin levels.[39] Synthesis of amino acids also had a beneficial effect on metabolic health and weight control of populations following the Western-style diet.[40] Leucine co-ingestion has been proposed to improve postprandial glycemia in patients with type 2 diabetes.[41] Thus, the results showed that GM dysfunction might lead to further susceptibility to HTN when one smoked. The imbalance of corresponding metabolites following these deficient microbial functions in amino acid biosynthesis, fatty acid utilization, and vitamin production might confer to the occurrence of CVD events in patients with HTN.

Although given emerging evidence showing the implication of smoking status in consequent GM dysbiosis and the causal role of intestinal microbiota in contributing to HTN development, our study was the first study to assess the profiles of GM in participants with smoking status and HTN. Moreover, the hypertensive patients were newly diagnosed and samples were collected prior to antihypertensive treatment. Last but not the least, gut microbial community was assessed by shotgun metagenomic sequencing, which allowed to be analyzed in species level and function level. However, there are also some limitations of this study. In our study, we failed to identify statistically remarkable difference in the α-diversity parameters which might be due to limited sample size. As the number of participants was relatively small in the current study, further studies with an expanded sample size to validate or further explore the difference between groups are still needed. In addition, the GM profiles of former smokers were not included in our study because of small sample size. Nevertheless, Lee SH et al[10] have investigated the relationship between smoking status and GM in never, former, and current smokers previously. They found no difference in GM composition between never and former smokers, including that GM of smokers would be restored by quitting smoking.

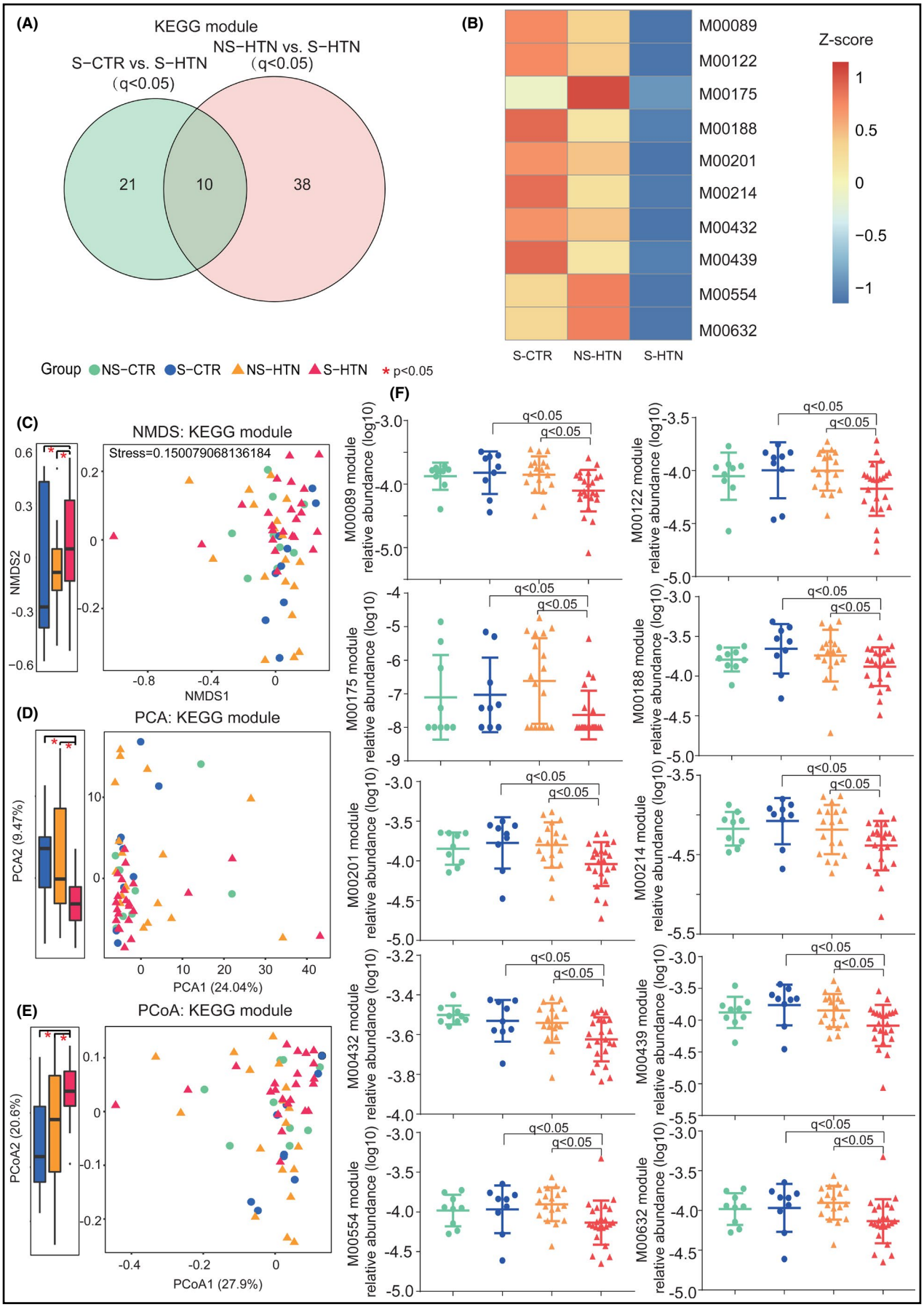
(A)
KEGG module
S−CTR vs. S−HTN (q<0.05)
NS−HTN vs. S−HTN (q<0.05)
21
10
38
(B)
M00089
M00122
M00175
M00188
M00201
M00214
M00432
M00439
M00554
M00632
S-CTR
NS-HTN
S-HTN
Z-score
1
0.5
0
−0.5
−1
Group NS−CTR S−CTR NS−HTN S−HTN * p<0.05
(C)
NMDS: KEGG module
Stress=0.150079068136184
NMDS1
NMDS2
(D)
PCA: KEGG module
PCA1 (24.04%)
PCA2 (9.47%)
(E)
PCoA: KEGG module
PCoA1 (27.9%)
PCoA2 (20.6%)
(F)
M00089 module relative abundance (log10)
M00122 module relative abundance (log10)
M00175 module relative abundance (log10)
M00188 module relative abundance (log10)
M00201 module relative abundance (log10)
M00214 module relative abundance (log10)
M00432 module relative abundance (log10)
M00439 module relative abundance (log10)
M00554 module relative abundance (log10)
M00632 module relative abundance (log10)
q<0.05

FIGURE 7 Fecal microbial gene functions significantly differently enriched between S-CTR and S-HTN, and between S-HTN and NS-HTN. (A) Venn diagrams showing the number of differential KEGG modules when comparing S-CTR and S-HTN, and NS-HTN and S-HTN. The overlap identified that 10 KEGG modules were shared; $q < 0.05$, Wilcoxon rank-sum test. (B) Heat map showing the 10 shared KEGG modules differently enriched in S-CTR, NS-HTN, and S-HTN. The abundance profiles were expressed by *Z* scores, and genera were clustered based on Bray-Curtis distance in the clustering tree. The *Z* score was negative (shown in blue) when the row abundance was lower than the mean and was shown in red when the row abundance was higher than the mean. (C–E) NMDS, PCA, and PCoA plots based on the relative abundance of KEGG modules in groups. Significant differences across groups were established at NMDS2, PCA2, and PCoA2, and are shown in the box plots. $^{*}p < .05$; $^{\#}p < .1$; Kruskal-Wallis test. (F) Scatter plots of the relative abundance of the 10 shared differential KEGG modules shared between S-HTN vs. S-CTR, and S-HTN vs. NS-HTN. In order to show it clear, the relative abundance of KEGG modules has been transformed into log10 values. Green, NS-CTR; cyan, S-CTR; yellow, NS-HTN; and orange, HTN-S. The dots indicate individual values of the participants, and the horizontal lines from the bottom to top represent 25th percentiles, medians, and 75th percentiles

5 | CONCLUSIONS

In conclusion, the findings of this study indicated a disorder induced by smoking based on exploring the dysbiotic intestinal flora in individuals with smoking status and HTN. Thus, smoking cessation was highlighted for hypertensive patients due to its potential in avoiding future CVD events through modulating GM.

CONFLICT OF INTEREST

All authors declare that they have no conflict of interest.

AUTHOR CONTRIBUTIONS

Pan Wang contributed to analysis, methodology, visualization, and writing—original draft preparation. Ying Dong contributed to methodology, software, writing—original draft preparation, reviewing, and editing. Jie Jiao contributed to investigation and visualization. Kun Zuo contributed to investigation and data curation. Chunming Han contributed to investigation. Lei Zhao contributed to validation. Shu Ding contributed to validation. Xinchun Yang contributed to resources. Mulei Chen contributed to conceptualization, supervision, reviewing, and editing. Jing Li contributed to conceptualization, methodology, supervision, project administration, writing—reviewing, and editing.

ORCID

Jing Li https://orcid.org/0000-0002-5102-4315

REFERENCES

1. Benjamin EJ, Virani SS, Callaway CW, et al. Heart disease and stroke statistics-2018 update: a report from the American Heart Association. *Circulation*. 2018;137(12):e67-e492. https://doi.org/10.1161/CIR.0000000000000558
2. Lewington S, Clarke R, Qizilbash N, et al. Age-specific relevance of usual blood pressure to vascular mortality: a meta-analysis of individual data for one million adults in 61 prospective studies. *Lancet*. 2002;360(9349):1903-1913. https://doi.org/10.1016/s0140-6736(02)11911-8
3. Lloyd-Jones DM, Larson MG, Leip EP, et al. Lifetime risk for developing congestive heart failure: the Framingham Heart Study. *Circulation*. 2002;106(24):3068-3072. https://doi.org/10.1161/01.cir.0000039105.49749.6f
4. Conen D, Tedrow UB, Koplan BA, Glynn RJ, Buring JE, Albert CM. Influence of systolic and diastolic blood pressure on the risk of incident atrial fibrillation in women. *Circulation*. 2009;119(16):2146-2152. https://doi.org/10.1161/circulationaha.108.830042
5. Klag MJ, Whelton PK, Randall BL, et al. Blood pressure and end-stage renal disease in men. *N Engl J Med*. 1996;334:13-18.
6. Mathers CD, Loncar D. Projections of global mortality and burden of disease from 2002 to 2030. *PLoS Med*. 2006;3:e442. https://doi.org/10.1371/journal.pmed.0030442
7. Primatesta P, Falaschetti E, Gupta S, Marmot MG, Poulter NR. Association between smoking and blood pressure: evidence from the health survey for England. *Hypertension*. 2001;37(2):187-193. https://doi.org/10.1161/01.hyp.37.2.187
8. Feng Q, Liang S, Jia H, et al. Gut microbiome development along the colorectal adenoma-carcinoma sequence. *Nat Commun*. 2015;6(1):6528. https://doi.org/10.1038/ncomms7528
9. Qin N, Yang F, Li A, et al. Alterations of the human gut microbiome in liver cirrhosis. *Nature*. 2014;513:59-64.
10. Lee SH, Yun Y, Kim SJ, et al. Association between cigarette smoking status and composition of gut microbiota: population-based cross-sectional study. *J Clin Med*. 2018;7(9):282. https://doi.org/10.3390/jcm7090282
11. Stewart CJ, Auchtung TA, Ajami NJ, et al. Effects of tobacco smoke and electronic cigarette vapor exposure on the oral and gut microbiota in humans: a pilot study. *PeerJ*. 2018;6:e4693. https://doi.org/10.7717/peerj.4693
12. Biedermann L, Zeitz J, Mwinyi J, et al. Smoking cessation induces profound changes in the composition of the intestinal microbiota in humans. *PLoS ONE*. 2013;8:e59260.
13. Gomez-Guzman M, Toral M, Romero M, et al. Antihypertensive effects of probiotics Lactobacillus strains in spontaneously hypertensive rats. *Mol Nutr Food Res*. 2015;59(11):2326-2336. https://doi.org/10.1002/mnfr.201500290
14. Khalesi S, Sun J, Buys N, et al. Effect of probiotics on blood pressure: a systematic review and meta-analysis of randomized, controlled trials. *Hypertension*. 2014;64(4):897-903. https://doi.org/10.1161/hypertensionaha.114.03469
15. Li J, Zhao F, Wang Y, et al. Gut microbiota dysbiosis contributes to the development of hypertension. *Microbiome*. 2017;5(1):14. https://doi.org/10.1186/s40168-016-0222-x
16. World Health Organization. *Guidelines for controlling and monitoring the tobacco epidemic*. Geneva: World Health Organization; 1998: 76–101. http://apps.who.int/iris/bitstream/handle/10665/42049/9241545089-eng.pdf?sequence=8
17. Zeller G, Tap J, Voigt AY, et al. Potential of fecal microbiota for early-stage detection of colorectal cancer. *Mol Syst Biol*. 2014;10:766.
18. Yuzefpolskaya M, Bohn B, Nasiri M, et al. Gut microbiota, endotoxemia, inflammation, and oxidative stress in patients with heart failure, left ventricular assist device, and transplant. *J Heart Lung Transplant*. 2020;39(9):880-890. https://doi.org/10.1016/j.healun.2020.02.004
19. Arumugam M, Raes J, Pelletier E, et al. Enterotypes of the human gut microbiome. *Nature*. 2011;473(7346):174-180. https://doi.org/10.1038/nature09944

20. Huson DH, Auch AF, Qi J, et al. MEGAN analysis of metagenomic data. *Genome Res*. 2007;17(3):377-386. https://doi.org/10.1101/gr.5969107
21. Backhed F, Roswall J, Peng Y, et al. Dynamics and stabilization of the human gut microbiome during the first year of life. *Cell Host Microbe*. 2015;17(5):690-703. https://doi.org/10.1016/j.chom.2015.04.004
22. Tilg H, Kaser A. Gut microbiome, obesity, and metabolic dysfunction. *J Clin Invest*. 2011;121:2126-2132.
23. Tang WH, Kitai T, Hazen SL. Gut microbiota in cardiovascular health and disease. *Circ Res*. 2017;120:1183-1196.
24. Howitt MR, Garrett WS. A complex microworld in the gut: gut microbiota and cardiovascular disease connectivity. *Nat Med*. 2012;18:1188-1189.
25. Backhed F, Ley RE, Sonnenburg JL, et al. Host-bacterial mutualism in the human intestine. *Science*. 2005;307(5717):1915-1920. https://doi.org/10.1126/science.1104816
26. Xu J, Gordon JI. Honor thy symbionts. *Proc Natl Acad Sci USA*. 2003;100:10452-10459.
27. Guinane CM, Cotter PD. Role of the gut microbiota in health and chronic gastrointestinal disease: understanding a hidden metabolic organ. *Therap Adv Gastroenterol*. 2013;6:295-308.
28. Ley RE, Turnbaugh PJ, Klein S, et al. Microbial ecology: human gut microbes associated with obesity. *Nature*. 2006;444(7122):1022-1023. https://doi.org/10.1038/4441022a
29. Ley RE, Backhed F, Turnbaugh P, et al. Obesity alters gut microbial ecology. *Proc Natl Acad Sci USA*. 2005;102:11070-11075.
30. Turnbaugh PJ, Ley RE, Mahowald MA, et al. An obesity-associated gut microbiome with increased capacity for energy harvest. *Nature*. 2006;444(7122):1027-1031. http://dx.doi.org/10.1038/nature05414
31. Chen W, Liu F, Ling Z, et al. Human intestinal lumen and mucosa-associated microbiota in patients with colorectal cancer. *PLoS ONE*. 2012;7:e39743.
32. Sivaprakasam S, Gurav A, Paschall AV, et al. An essential role of Ffar2 (Gpr43) in dietary fibre-mediated promotion of healthy composition of gut microbiota and suppression of intestinal carcinogenesis. *Oncogenesis*. 2016;5:e238. https://doi.org/10.1038/oncsis.2016.38
33. Elinav E, Strowig T, Kau AL, et al. NLRP6 inflammasome regulates colonic microbial ecology and risk for colitis. *Cell*. 2011;145(5):745-757. https://doi.org/10.1016/j.cell.2011.04.022
34. Chow J, Tang H, Mazmanian SK. Pathobionts of the gastrointestinal microbiota and inflammatory disease. *Curr Opin Immunol*. 2011;23:473-480.
35. Kelly TN, Bazzano LA, Ajami NJ, et al. Gut microbiome associates with lifetime cardiovascular disease risk profile among bogalusa heart study participants. *Circ Res*. 2016;119(8):956-964. https://doi.org/10.1161/CIRCRESAHA.116.309219
36. Boursier J, Mueller O, Barret M, et al. The severity of nonalcoholic fatty liver disease is associated with gut dysbiosis and shift in the metabolic function of the gut microbiota. *Hepatology*. 2016;63:764-775.
37. Chun SJ, Cui Y, Ahn CY, et al. Improving water quality using settleable microalga Ettlia sp. and the bacterial community in freshwater recirculating aquaculture system of Danio rerio. *Water Res*. 2018;135:112-121. https://doi.org/10.1016/j.watres.2018.02.007
38. De Cesare A, Sala C, Castellani G, et al. Effect of Lactobacillus acidophilus D2/CSL (CECT 4529) supplementation in drinking water on chicken crop and caeca microbiome. *PLoS ONE*. 2020;15:e0228338.
39. Rowland I, Gibson G, Heinken A, et al. Gut microbiota functions: metabolism of nutrients and other food components. *Eur J Nutr*. 2018;57(1):1-24. https://doi.org/10.1007/s00394-017-1445-8
40. Bifari F, Ruocco C, Decimo I, et al. Amino acid supplements and metabolic health: a potential interplay between intestinal microbiota and systems control. *Genes Nutr*. 2017;12:27. https://doi.org/10.1186/s12263-017-0582-2
41. van Loon LJ. Leucine as a pharmaconutrient in health and disease. *Curr Opin Clin Nutr Metab Care*. 2012;15(1):71-77. https://doi.org/10.1097/mco.0b013e32834d617a

SUPPORTING INFORMATION

Additional supporting information may be found online in the Supporting Information section.

How to cite this article: Wang P, Dong Y, Jiao J, et al. Cigarette smoking status alters dysbiotic gut microbes in hypertensive patients. *J Clin Hypertens*. 2021;23:1431–1446. https://doi.org/10.1111/jch.14298